Active Control of Radial Rotor Vibrations in Electric Machines – Identification, Modeling and Control Design

Juha Orivuori, Antti Laiho, and Anssi Sinervo

***Abstract*— This paper presents results related to modeling, identification, control design and simulation of an electric motor equipped with a new force actuator. The model consists of several partial models, thus separating certain physical phenomena into independent processes. The inputs and outputs of the models to be identified are strongly correlated. This makes the identification process significantly more complicated. Three different control algorithms are designed for the process. The performance of the control algorithms are tested against finite element models in extensive simulations. The paper concludes in description of preliminary test results with an actual test machine.**

***Index Terms*— control design, electric motors, identification, modeling**

I. Introduction

The interest in suppressing rotor vibrations in electric machines is increasing all the time. Due to the nature of the process this goal can be met only through active vibration control, because passive and semi-active methods generate new vibrations on different operating frequencies, which is an unwanted phenomenon. The increased demands for vibration control arise from the increased miniaturization of the motors and for the purpose of higher efficiency. To meet these objectives the air-gap of the motor would be significantly smaller. Consequently, the vibrations have to be suppressed in order to minimize the variation in the air-gap length and to prevent possible collisions between the rotor and the stator. Another reason for vibration control is the reduced wear and tear of supportive structures and rotor bearings, resulting in decreased maintenance costs and downtimes. The vibration control also permits the use of the motor at all driving speeds as the resonance peaks are leveled out and the motor can be driven at the critical frequencies also. In general this would allow a more general motor design, opposed to motors designed solely for a single task, thus allowing mass production and shorter delivery times. All of these aspects may result in increased profits to the producers and decreased costs to the customers.

In this paper active control of radial rotor vibrations in a three-phase motor is considered. The control forces are excited on the rotor by a state of the art actuator that is implemented as additional windings in the stator slots. The general idea is to generate a magnetic field that can be controlled in such a way that the magnetic force excited on the rotor is in radial direction. Even when an additional magnetic field is generated, the actuator's geometry is designed such that it can be assumed to have no interference with the main magnetic field driving the motor. The focus in this paper is on the identification of the actuator dynamics, general model structure, control design and simulation.

II. Modeling

In order to implement a control law, the process to be controlled has to be modeled in some fashion. The phenomena acting in the process can here be divided into three clearly separate processes. The motor consists of rotor, stator and actuator windings. If only the rotor displacement is considered, the separate stator model can be excluded. It is assumed that the magnetic fields generated by the actuator do not interfere with the stator fields. The displacement is excited by some forces acting on the rotor. These forces can be divided into control forces that are generated for the purpose to suppress the displacement and into disturbance forces that are uncontrollable. Therefore the motor model can be expressed as a composition of the rotor, actuator and disturbance models interacting with each other. This approach has many benefits as the model is highly modular. Therefore, if for some reason, the dynamics of a partial model change, it affects only that particular model and the structure of the control algorithms remain unchanged. This permits the reuse of the pre-made algorithms on different processes with the same structure but different dynamics.

A. Rotor model

The rotor model represents the mechanical dynamics of the motor. The model describes the relationship between the force acting on the rotor and the resulting displacement. As far as

J. Orivuori is with the Department of Automation and Systems Technology, Helsinki University of Technology, Finland

A. Laiho is with the VTT, Technical Research Centre of Finland, Finland

A. Sinervo is with the Department of Electrical Engineering, Helsinki University of Technology, Finland

the control of vibrations is considered, the most interesting parts of the model are its natural frequencies and their corresponding damping ratios. If a force is excited on the rotor at this frequency the resulting displacement is significantly higher.

One way to achieve a model for the rotor is to derive it from structural FE models of the motor components and then reduce it to the *n* lowest mode shapes and their corresponding eigenfrequencies. The dynamics of a rod in two dimensions can be described with a particular set of sine waves with different frequencies – mode shapes. The resulting model can be expressed as [1]:

$$\begin{aligned} \ddot{\eta} + 2\Xi\Omega\dot{\eta} + \Omega^2\eta &= \Phi_{rc}^T f_c + \Phi_{rc}^T f_{ex} \\ u_{rc} &= \Phi_{rc}\eta \end{aligned}, \qquad (1)$$

where η is the modal coordinate vector, Ω is a matrix containing the natural frequencies of the system, Ξ is a matrix containing the damping coefficients for each of the frequencies, Φ_{rc} is a sub-matrix of Φ that contains the mass-normalized mode shapes for each η, f_c is the control force and f_{ex} is the disturbance force.

Another way of achieving the rotor model is to express it as a Jeffcott rotor, which is the simplest model for a rotor [2]. The Jeffcott rotor can be considered as a disc attached to a weightless and flexible shaft with rigid supports Fig. 1.

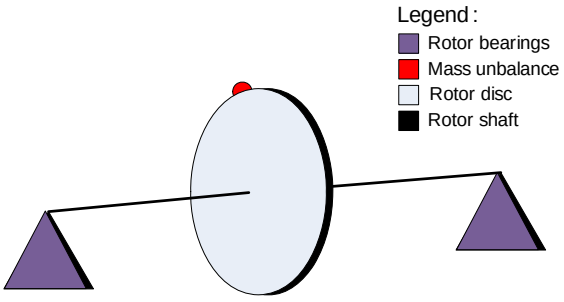

Fig. 1 A sketch of Jeffcott-rotor

The disc is symmetric with respect to its rotation axis except for a single point on the exterior of the disc that can be considered as a mass unbalance or the point of excitation for external forces Fig. 2. The shaft can be interpreted as a spring and a damper opposing displacement of the disc. This can be described with the general one degree of freedom spring-mass-damper-system [3]:

$$m\ddot{x}(t) + c\dot{x}(t) + kx(t) = K(u(t) + d(t)), \qquad (2)$$

where *m* is the mass of the rotor disc, *c* is the damping coefficient of the shaft, *k* is the spring constant of the shaft, *u(t)* is the control force, *K* is the system gain, *x(t)* is the rotor displacement and *d(t)* is the disturbance force.

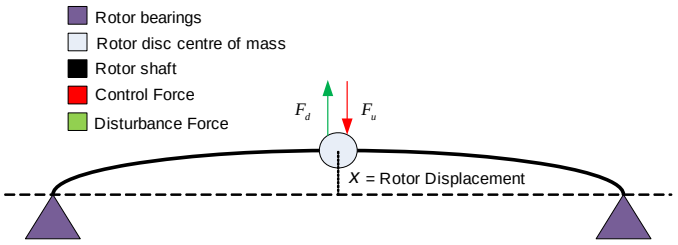

Fig. 2 Projection of the rotor position in a single plane

This model describes only one plane in the Cartesian coordinates, thus another similar model is needed to describe the rotor in three dimensions. The characteristics of the bearings are assumed to be similar in all directions and the dynamics in x- and y-coordinates are independent of each other, thus the final model can be expressed as:

$$\begin{cases} \dot{x}(t) = \begin{bmatrix} -2\zeta\omega_n & 1 & 0 & 0 \\ -\omega_n^2 & 0 & 0 & 0 \\ 0 & 0 & -2\zeta\omega_n & 1 \\ 0 & 0 & -\omega_n^2 & 0 \end{bmatrix} x(t) + \begin{bmatrix} 0 & 0 \\ \omega_n^2 & 0 \\ 0 & 0 \\ 0 & \omega_n^2 \end{bmatrix} d(t) + \begin{bmatrix} 0 & 0 \\ \omega_n^2 & 0 \\ 0 & 0 \\ 0 & \omega_n^2 \end{bmatrix} u(t) \\ y(t) = \begin{bmatrix} 1 & 0 & 0 & 0 \\ 0 & 0 & 1 & 0 \end{bmatrix} x(t) \end{cases}, \qquad (3)$$

where ω_n is the natural frequency and ζ is the damping ratio of the rotor.

A general presentation for the rotor model can be expressed as:

$$\begin{cases} \underset{mx1}{\dot{x}_r(t)} = \underset{mxm}{A_r}\ \underset{mx1}{x_r(t)} + \underset{mx2}{B_r}\ \underset{2x1}{u_r(t)} + \underset{mx2}{B_r}\ \underset{2x1}{d(t)} \\ \underset{2x1}{y_r(t)} = \underset{2xm}{C_r}\ \underset{mx1}{x_r(t)} \end{cases}. \qquad (4)$$

Both models behave approximately in the same fashion, and the latter and simpler one is chosen for use.

B. *Disturbance model*

The disturbance force acting on the rotor is generated by the mass-unbalance of the rotor. This force has a high correlation with the angular velocity of the rotor, the higher the velocity the stronger the force. The net disturbance force can be separated into two independent forces acting in x- and y-directions. Each of these partial forces can be expressed as a sinusoidal wave with the same frequency as the rotation speed of the rotor. The amplitude of the force depends on the characteristics of the rotor. The dynamics of the sinusoidal wave can be solved by differentiation:

$$y(t) = A\sin(\omega_d t + n\frac{\pi}{2})$$
$$\dot{y}(t) = A\omega_d \cos(\omega_d t + n\frac{\pi}{2}) \quad , \tag{5}$$
$$\ddot{y}(t) = -A\omega_d^2 \sin(\omega_d t + n\frac{\pi}{2})$$

where A is the amplitude of the wave, ω_d is the angular frequency of the wave and n is zero for a sine wave and unity for a cosine wave.

With some manipulations [4] this yields a general model for disturbance acting in one direction:

$$\begin{cases} \underset{2x1}{\dot{w}(t)} = \underset{2x2}{\begin{bmatrix} 0 & 1 \\ -\omega_d^2 & 0 \end{bmatrix}} \underset{2x1}{w(t)} \\ \underset{1x1}{v(t)} = \underset{1x2}{\begin{bmatrix} 1 & 0 \end{bmatrix}} \underset{2x1}{w(t)} \end{cases} . \tag{6}$$

A general model for the total disturbance is achieved by combining two separate disturbance models (6):

$$\begin{cases} \underset{4x1}{\dot{x}_d(t)} = \underset{4x4}{A_d}\ \underset{4x1}{x_d} = \underset{4x4}{\begin{bmatrix} 0 & 1 & 0 & 0 \\ -\omega_x^2 & 0 & 0 & 0 \\ 0 & 0 & 0 & 1 \\ 0 & 0 & -\omega_y^2 & 0 \end{bmatrix}} \underset{4x1}{x_d(t)} \\ \underset{2x1}{d(t)} = \underset{2x4}{C_d}\ \underset{4x1}{x_d} = \underset{2x4}{\begin{bmatrix} 1 & 0 & 0 & 0 \\ 0 & 0 & 1 & 0 \end{bmatrix}} \underset{4x1}{x_d(t)} \end{cases} . \tag{7}$$

The model has no inputs as it is assumed to be excited with some initial impulse. This can be achieved by setting the initial states as:

$$x_d(0) = \begin{bmatrix} 0 \\ A_x\omega_x \\ A_y \\ 0 \end{bmatrix} \tag{8}$$

C. Actuator model

The actuator model describes the electrical system generating the control forces. The force generation of the actuator has high dependency on the position of the rotor as the strength of the magnetic field is proportional to the width of the air-gap. Thus, the model has two input pairs, one for the control voltage and one for the rotor position. It turns out that the rotor position is actually the dominating parameter. A set of differential equations describing the system has been derived [1], yielding:

$$f_c = \frac{\pi d_r l_r}{4\mu_0\delta_0}(B_p^2 z_r + \mu_0(K_{r,p-1}B_p\hat{i}^*_{r,p-1,0} + K_{r,p+1}B_p^*\hat{i}_{r,p+1,0} + K_{c,p+1}B_p^*\hat{i}_{c,p+1,0}))$$
$$\hat{U}_{c,p+1,0} = (R_{c,p+1} + j\omega_1(L_{c,p+1} + M_{r,c,p+1}))\hat{i}_{c,p+1,0} + M_{r,c,p+1}\frac{d\hat{i}_{r,p+1,0}}{dt} + L_{c,p+1}\frac{d\hat{i}_{c,p+1,0}}{dt} \tag{9}$$
$$L_{r,p+1}\frac{d\hat{i}_{r,p+1,0}}{dt} + (R_{r,p+1} + j\omega_{p+1}L_{r,p+1})\hat{i}_{r,p+1,0} + j\omega_{p+1}M_{r,c,p+1}\hat{i}_{c,p+1,0}$$
$$+ M_{r,c,p+1}\frac{d\hat{i}_{c,p+1,0}}{dt} + \frac{Lk_{r,p+1}}{2\mu_0}B_p(\dot{z}_r + j\omega_{p+1}z_r) = 0$$
$$L_{r,p-1}\frac{d\hat{i}^*_{r,p-1,0}}{dt} + (R_{r,p-1} - j\omega_{p-1}L_{r,p-1})\hat{i}^*_{r,p-1,0} + \frac{LK_{r,p-1}}{2\mu_0}B_p^*(\dot{z}_r - j\omega_{p-1}z_r) = 0$$

where subscripts p and $p\pm1$ are spatial harmonics of the main magnetomotive force (MMF) in the air-gap, r and c denote the rotor cage and control winding, respectively, * denotes a complex-conjugate, f_c is the force produced by the actuator and z_r is the coordinate vector of the rotor.

This is an exact model of the physical system. Unfortunately the model is quite complicated so it cannot be used for traditional control design. The model was manipulated further in order to transform it into a linear state-space presentation:

$$\begin{cases} \underset{nx1}{\dot{x}_a(t)} = \underset{nxn}{A_a}\ \underset{nx1}{x_a(t)} + \underset{nx2}{B_{a1}}\ \underset{2x1}{u_a(t)} + \underset{nx2}{B_{a2}}\ \underset{2x1}{y_r(t)} \\ \underset{2x1}{y_a(t)} = \underset{2xn}{C_a}\ \underset{nx1}{x_a(t)} \end{cases} . \tag{10}$$

The parameters of this model are unknown and do not have any clear physical meaning. This problem is solved by identifying the parameters from a model describing the system. This FE model [5] corresponds with the original model (9).

D. Model Aggregation

In order to acquire a model describing the whole process, the partial models have to be combined. The couplings between the models are shown in Fig. 3.

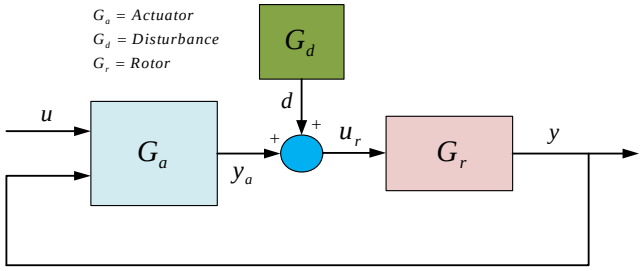

Fig. 3 Couplings between motor sub-models

The complete model of the process with the disturbances

included can be presented as:

$$\begin{cases} \underset{(m+n+4)x1}{\dot{x}(t)} = \underbrace{\begin{bmatrix} A_r & B_r C_a & B_r C_d \\ B_{a2} C_r & A_a & 0 \\ 0 & 0 & A_d \end{bmatrix}}_{(m+n+4)x(m+n+4)} \underset{(m+n)x1}{x(t)} + \underbrace{\begin{bmatrix} 0 \\ B_{a1} \\ 0 \end{bmatrix}}_{(m+n+4)x4} \underset{4x1}{u(t)} \\ \underset{2x1}{y(t)} = \underbrace{\begin{bmatrix} C_r & 0 & 0 \end{bmatrix}}_{2x(m+n+4)} \underset{(m+n+4)x1}{x(t)} \end{cases}, \quad (11)$$

where $y(t)$ is the rotor displacement, $u(t) = u_a(t)$ and $x(t) = \begin{bmatrix} x_r(t) \\ x_a(t) \\ x_d(t) \end{bmatrix}$.

III. Identification

As stated earlier, the actuator model has to be identified. An FE model for the actuator already exists, but unfortunately the model is heavy to calculate. The problems in the calculation make the simulation of the process very slow, thus testing different control designs would be a very time consuming process. The solution to this problem is to identify a linear model from the input-output data received by simulating the FE model. Naturally this is exactly the same process that has to be made on the actual test rig.

There exists a wide variety of different identification algorithms [6] of which prediction error method (PEM) for state-space models turned out to provide the best results. The identification procedure can be divided into three separate phases: data acquisition, model fitting and model validation.

A. Data acquisition

The data for the identification is acquired through simulation of the FE model. The model has two input pairs, one for the control voltage and one for the rotor position. As the data is acquired through simulation, arbitrary inputs can be used, which is seldom the case in real processes. The input range for the voltages is ±14V and 200µm for the displacements.

The voltages fed into the model are chosen to be pseudorandom signals limited to ±1V. The PRS was used as it guarantees that the signal is rich enough, thus exciting most of the frequencies of the system and yielding the best model performance for a generalized model. The absolute value of the signal is limited to 1V as the FE model is non-linear and it may saturate at the maximal voltages. The saturation would lead into biased output, which would corrupt the identified model.

The best choice for the displacements fed into the model would naturally be PRS signals as well. Unfortunately it turns out that the actuator is a stiff process, this prohibits the use of PRS signal as it would only get filtered out. One solution would be the use of the output of the rotor model having the outputs of the actuator as its inputs. This solution however yields even worse results, due to two reasons. First of all the frequency content of the rotor output is not rich enough; therefore most of the frequencies of the actuator are never excited. Secondly there is linear relationship between the actuator input and the rotor output, which is typical to many processes. This results into infinite number of solutions for the problem. The solution for this problem is to use the output of the rotor model as input and modulating it with PRS signal with amplitude of 10% of the amplitude of the original signal, Fig. 4. This breaks the linear dependencies and is rich enough to excite most of the frequencies of the system.

The sampling rate for the data has to be chosen carefully to prevent aliasing. According to Shannon's Theorem [7] the sampling frequency should be at least:

$$\omega_s = 2\omega_n, \quad (12)$$

where ω_s is sampling frequency in radians/sec and ω_n is the Nyquist frequency.

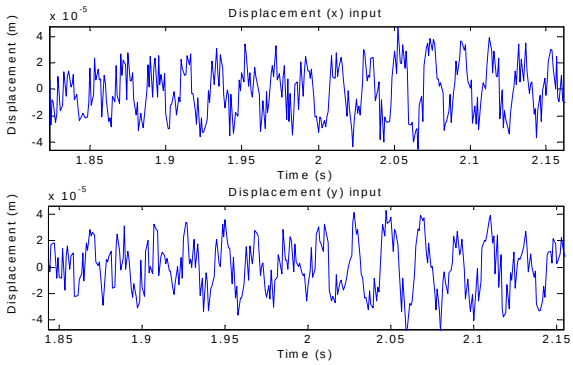

Fig. 4 Rotor displacements used in the identification with 10% noise modulation

The Nyquist frequency is approximately the same as the frequency of the fastest dynamic mode of the system. The sampling rate should be only as fast as needed. Is the sampling rate is too high, the system behaves as an integrator and all the dynamics are lost, thus preventing identification. According to a priori knowledge it is known that the most interesting phenomena occur below 100Hz, thus the sampling rate is chosen to be 1 kHz.

B. Identification process

The first phase in the identification is to divide the data into training and validation data. This is a very important phase as if this step is omitted the resulting model may seem to have an excellent performance, while in reality it does not describe the original system well. This is due to overfitting of the model, the model tries to describe the data too accurately, thus

performing curve fitting instead of describing the actual dynamics of the system.

After the data is divided it will be preprocessed. This procedure significantly enhances the identification results. In preprocessing the initial transients are removed and the data is set to zero mean and normalized between ±1. As there is no information on the order of the system, few guesses are made. If the system has cancellable pole-zero pairs the order is too high. Naturally the order should be selected only as high as necessary for good results. The more states the process has the harder it is to design an effective control law due to some potential numerical problems.

C. *Model validation*

The acquired model has to be validated against data that was not used in the identification. This guarantees that the model is actually a general model of the system, not just a fit of the data. Fortunately another completely different set of data was available that was used for subspace identification (SUB). This data provides the best validation capabilities as it is completely independent.

The model should be validated both in the time and frequency domain to guarantee the best performance. The time domain validation is shown in Fig. 5 and Fig. 6. The frequency domain analysis is presented in Fig. 7 and Fig. 8. It is apparent, that the models have a good fit and thus represent a good approximation of the system.

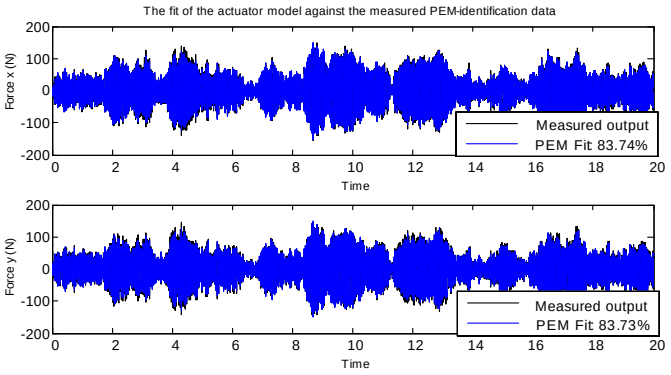

Fig. 5 Comparison of the PEM-identified actuator against the PEM-identification data

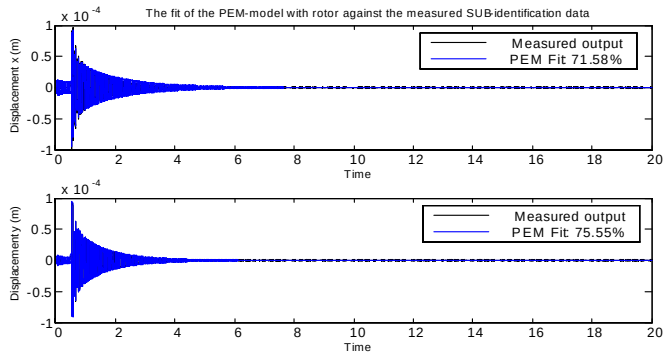

Fig. 6 Comparison of the PEM-identified model with rotor against the SUB-identification data

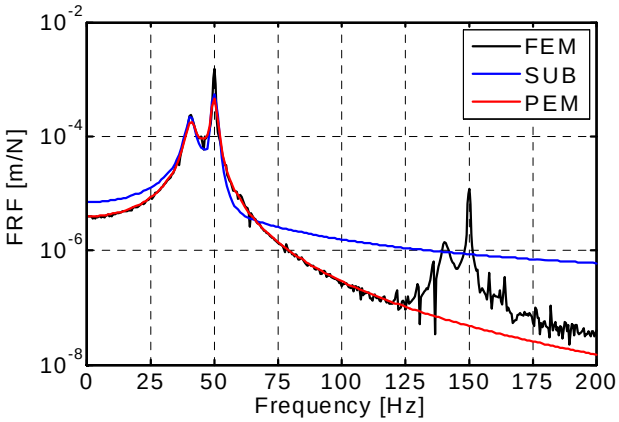

Fig. 7 Gain comparison of the SUB- and PEM-identified models against the measured output

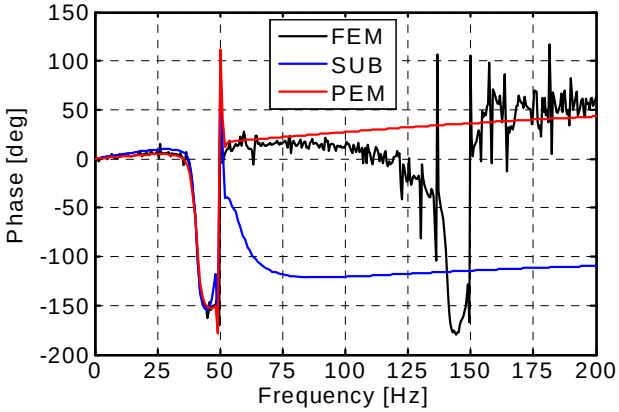

Fig. 8 Phase comparison of the SUB- and PEM-identified models against the measured output

IV. Control Design

Three different control algorithms are designed for the process and then compared with each other. The analysis of the process [4] points out that the control algorithm must have some prediction capabilities in order to suppress the dynamic disturbance. The control algorithms implemented are: an augmented LQ-controller, convergent controller and a modified adaptive controller.

A. *LQ-controller*

An augmented LQ-controller was designed for the process [4]. The controller is augmented with states representing the integral of the net forces acting on the rotor. Therefore, in order to minimize the cost, this force has to be minimized. Because the LQ-controller is a state-feedback controller a state-observer has to be designed. After the vector containing the control weights and state-observer are designed, they are combined into a single controller as shown in Fig. 9.

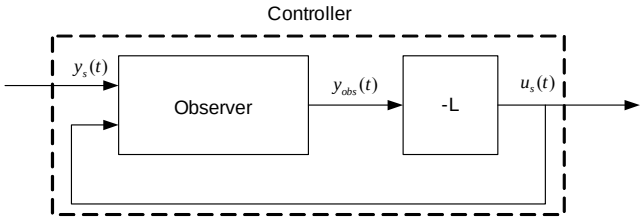

Fig. 9 Relations between state-observer and the state-controller forming the actual controller

The resulting controller can be expressed as:

$$\begin{cases} \dot{x}_{cont}(t) = \begin{bmatrix} \dot{x}_{obs}(t) \\ \hline \dot{x}_{aug}(t) \end{bmatrix} = \left[\begin{array}{c|c} A_{obs} - B_s L_{obs} C_{obs} & -B_s L_{aug} \\ \hline A_{aug} & I \end{array}\right] x_{cont}(t) + \begin{bmatrix} K \\ \hline 0 \end{bmatrix} u_{cont}(t) \\ y_{cont}(t) = -L x_{cont}(t) \end{cases}, \quad (13)$$

where $u_{cont}(t)$ is the rotor displacement, $y_{cont}(t)$ is the control-signal for the process, subscripts *obs*, *cont* and *aug* indicate the observer, controller and augmented state models and L is a partitioned matrix $L_{2x20} = \left[\begin{array}{c|c} L_{obs} & L_{aug} \\ {\scriptstyle 2x18} & {\scriptstyle 2x2} \end{array}\right]$.

B. Convergent Control

Convergent control algorithm [2] is a feedforward compensation method that uses an integrating adaptation law. The control design is a cascaded controller that has a traditional feedback-controller in the inner loop and the convergent controller in the outer loop as in Fig. 10.

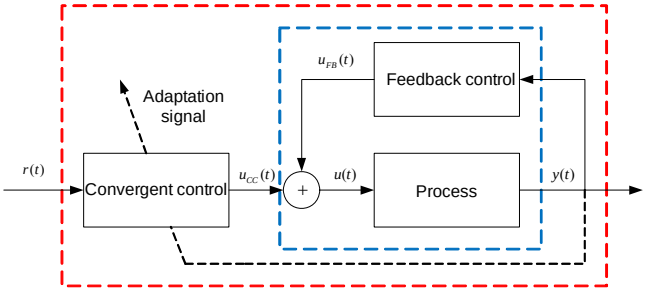

Fig. 10 Cascaded controller layout used for convergent control

The control law is achieved by minimizing a quadratic cost function:

$$U_F = -(\hat{G}_F^H \hat{G}_F)\hat{G}_F^H D_F = -A_F D_F, \quad (14)$$

where $\hat{G}_F$ is the estimated complex frequency response of the system and D_F is the Fourier coefficient of the disturbance.

The adaptive control law can be written as:

$$U_F(n+1) = [\gamma I - \alpha A_F G_F] U_F(n) - \alpha A_F D_F(n), \quad (15)$$

where γ is a positive number below unity called *leak coefficient* and α is a positive number called *convergence coefficient*.

C. Modified adaptive controller

The control signal in this method is generated created by using the inverse of the actuator model at a specific frequency. The details on the algorithm can be found in [8].

The adaptive control law in frequency domain can be written as:

$$U(k+1) = U(k) - K_u(M_a^{-1}(D_\omega(k) + K_{ud}(D_\omega(k) + Y_{a,\omega}(k))) + U(k)), \quad (16)$$

where K_u is a Kalman gain, K_{ud} is coefficient for the convergent part of the control law, $D_\omega(k)$ is the estimate of the disturbance forces, M_a is the transfer function matrix of the actuator and $Y_{a,\omega}(k)$ is the rotor displacement in polar coordinate basis.

V. Simulations

The performance of the designed control laws are validated by simulations. The simulations are carried out with a model that uses the non-linear FE model combined with the rotor and disturbance models as in Fig. 11. The simulations are made in Matlab Simulink. The process model is simulated as continuous system controlled with a discrete controller with sampling frequency of 1000 Hz. It is obvious that the controllers should perform pretty well with the exact models. However the simulated actuator model is non-linear, while the model used for control design was linear. This brings some model error into the simulation, which is good in the validation point of view.

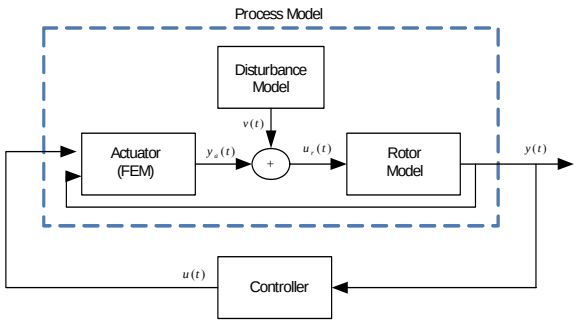

Fig. 11 Block-diagram of the controlled system used in the simulations

In simulation the process is first run without control. After a while the controller is turned on, making the impact and performance clearly visible. The simulation results for different controllers can be seen in following figures. Fig. 12, Fig. 14 and Fig. 16 represent the rotor displacement in x-direction, due to the symmetry of the system it is almost

identical to the displacement in y-direction. Fig. 13, Fig. 15 and Fig. 17 represent the control voltages fed into the actuator. Fig. 18, Fig. 19 and Fig. 20 illustrate the rotor displacement in xy-plane. It turns out that each of the controllers performs in a quite similar fashion. The displacements caused by the disturbance forces have been suppressed to 3% of their original amplitude. These results are not amplitude dependent. The mean value of the control voltage fed into the actuator is approximately 0,15 volts while the limit was 14 volts. Under these results it is obvious that the control algorithms are performing very well.

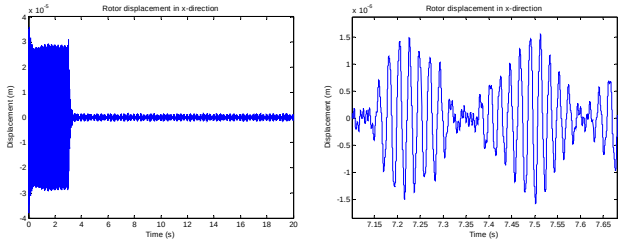

Fig. 12 Rotor displacement in x-direction with LQ-controller

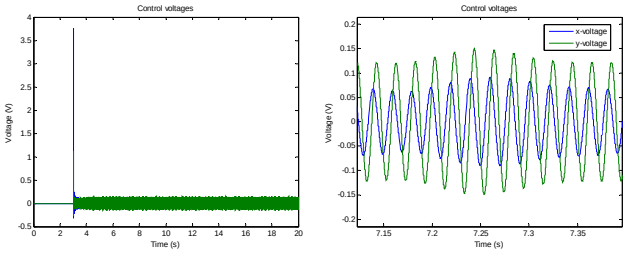

Fig. 13 Control voltage fed into the actuator with LQ-controller

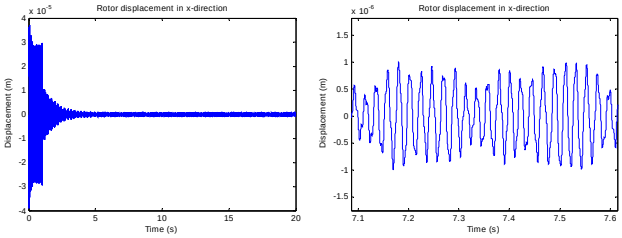

Fig. 14 Rotor displacement in x-direction with convergent controller

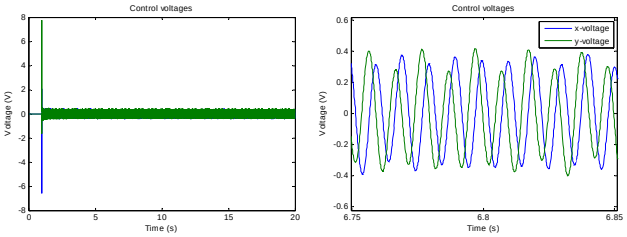

Fig. 15 Control voltage fed into the actuator with convergent controller

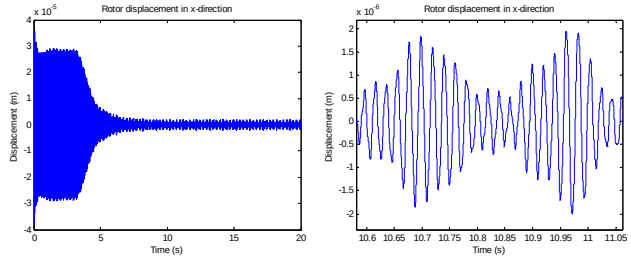

Fig. 16 Rotor displacement in x-direction with modified adaptive controller

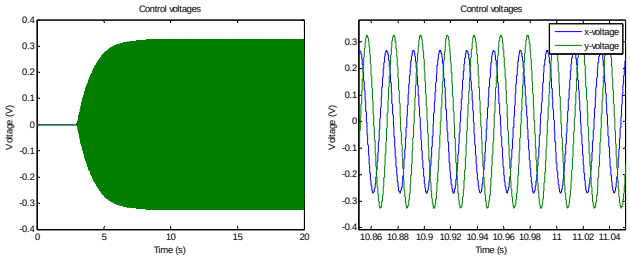

Fig. 17 Control voltage fed into the actuator with modified adaptive controller

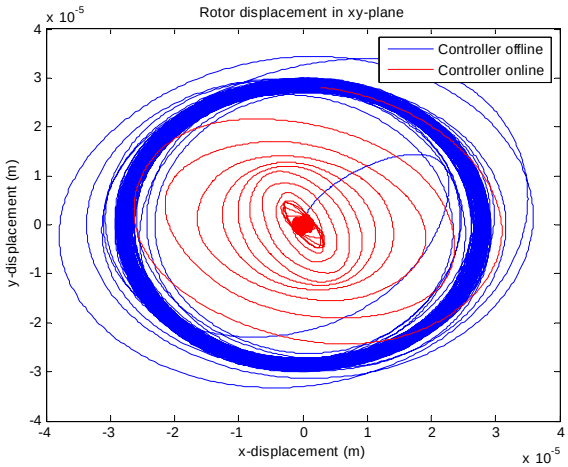

Fig. 18 Rotor displacement in xy-plane with LQ-controller. Initially with the controller offline (blue) and later switched online (red)

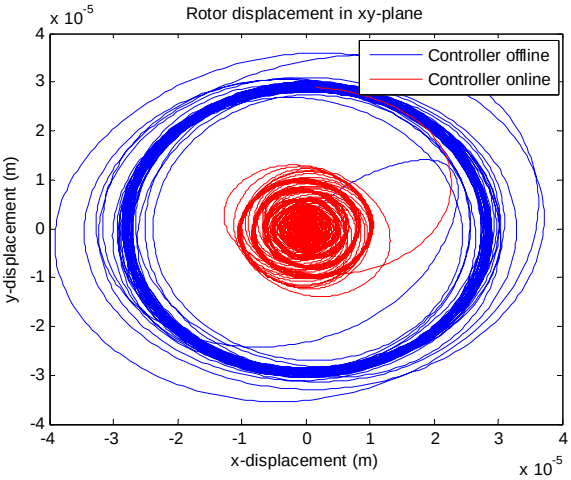

Fig. 19 Rotor displacement in xy-plane with convergent controller controller. Initially with the controller offline (blue) and later switched online (red)

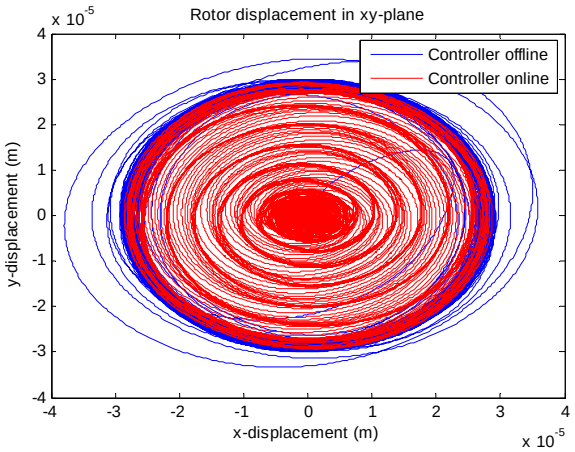

Fig. 20 Rotor displacement in xy-plane with modified adaptive controller. Initially with the controller offline (blue) and later switched online (red)

VI. Conclusions and Current Work

The modeling and control design of an electric motor are possible with the traditional identification and design methods. Dynamic disturbance is quite problematic for the control design, leading to the use of augmented and manipulated models. According to the simulations it is clear that the rotor displacement can be controlled with ease, resulting in significant decrease of vibrations. Three completely different control algorithms were implemented and all of them performed equally well.

The simulations are however never adequate. The actual processes tend to have dynamics that have not been modeled and may corrupt the control effort. The control algorithms presented here are being implemented on to a test motor. It has turned out in the preliminary tests that a controllable force can be generated with the actuator windings and the rotor model is approximately the same as the one presented in this paper. The identification of the actuator is significantly more difficult. The model structure presented here is good, but the amplitude of the disturbance forces is so high that the identification data is corrupted. Even as it is somewhat harder to identify the models it is possible. As long as no model with adequate accuracy exists the LQ- and adaptive controllers can not be implemented on the process. Convergent control was implemented and tested with inaccurate models. The control resulted into approximately 80% decrease in vibrations. Thus it is evident that the methods and designs presented in this paper will perform well with an actual test machine if the model is accurate enough.

Acknowledgement

The results presented in this paper are achieved as part of ACRVEM (Active Control of Rotor Vibrations in Electric Machines) - project funded by the Academy of Finland.

References

[1] Laiho, A., Tammi, K., Zenger, K., Arkkio, A. 2008, A model-based flexural rotor vibration control in cage induction machines by a built-in force actuator, *Archiv für Elektrotechnik* (available at: http://www.springerlink.com/content/x1166487r46432k 3)

[2] Tammi, K. 2007, *Active control of radial rotor vibrations : identification, feedback, feedforward, and repetitive control methods*, VTT Publications: 634, Doctoral Dissertation (available at:: http://www.vtt.fi/inf/pdf/publications/2007/P634.pdf)

[3] Inman, D.J. 2006, *Vibration with control*, Wiley, Hoboken, NJ.

[4] Orivuori, J., 2008, *Active Control of Rotor Vibrations in Electric Drives*, M.Sc. thesis, Department of Automation and Systems Technology, Helsinki University of Technology

[5] Arkkio, A. 1987, *Analysis of induction motors based on the numerical solution of the magnetic field and circuit equations*, Acta Polytechnica Scandinavica, Electrical Engineering Series No. 59, Doctoral Dissertation (available at: http://lib.tkk.fi/Diss/198X/isbn951226076X/).

[6] Ljung, L. 1999, *System identification : theory for the user*, 2nd edition, Prentice Hall, Upper Saddle River NJ.

[7] Oppenheim, A.V., Willsky, A.S. & Young, I.T. 1983, *Signals and systems*, Prentice-Hall, Englewood Cliffs, NJ.

[8] Zenger, K., Sinervo, A., Orivuori, J., Laiho, A., Tammi, K., Parallel disturbance compensator for electrical machines. To appear in the 17th *IFAC World Congress* (IFAC WC 2008).